Int. J. Multiphase Flow Vol. 14, No. 6, pp. 787–800, 1988
Printed in Great Britain.

0301-9322/88 $3.00 + 0.00

PARTICLE DISPERSION IN A SINGLE-SIDED BACKWARD-FACING STEP FLOW

B. RUCK and B. MAKIOLA

Forschungsgruppe Zweiphasenströmungen, Institut für Hydromechanik, Universität Karlsruhe, Kaiserstr. 12, 7500 Karlsruhe 1, B.R.D.

(*Received* 18 *April* 1988; *in revised form* 11 *July* 1988)

Abstract—The paper describes the particle dispersion in a single-sided backward-facing step flow. Particles of well-known sizes in the diameter range from 1 to 70 μm were suspended in an air flow and the particle motion over a step was measured by mean of a laser-Doppler anemometer. Thus, the local and integral flow quantities, i.e. the mean and turbulent velocity data could be measured precisely. In the experiments, monodispersed particle size distributions were used to exclude particle size related information ambiguity, known as triggering effects or size bias. The results of this study show qualitatively and quantitatively the difference in time-averaged particle dynamics for selected particle sizes in a backward-facing step flow. The experiments show, for different sizes, the changes in the particle velocity field in comparison with the velocity field of the continuous phase deduced from the 1 μm particles, and also imply the strong influences which different particle sizes have on flow data evaluation when size effects are not taken into account with particle-related optical measuring techniques.

Key Words: particle dispersion, step flow, flow separation

INTRODUCTION

To study the physics of flow separation, the asymmetrical backward-facing step flow provides a classic practical example. The simple geometry and the easily attainable two-dimensionality of the test flow facilitate the analysis of separation-induced flow phenomena, i.e. the determination of reattachment length or dividing streamlines. Thus, a great number of detailed studies (e.g. Abbott & Kline 1962; Bradshaw & Wong 1972; Nakagawa & Nezu 1987) have been published in the past on backward-facing single-sided step flows which describe the interactions of limiting geometrical parameters and flow characterizing quantities mostly in a time-averaged version. The influence of the boundary layer thickness on reattachment lengths of the flow and pressure distribution measurements has been studied intensively (e.g. Adams & Johnston 1988; Schmitt 1987). Experimental and numerical findings (see Armaly *et al.* 1983) were reported to be in good agreement for those Reynolds numbers for which the flow maintains its two-dimensionality.

Particle-laden flows with separation can be found in many technical and environmental processes and a better understanding of the particle dynamics can increase the efficiency of technical equipment. For the estimate of erosion potentials, e.g. in wall-bounded flows with a sudden change of wall geometry as, for example, caused by steps or welding seams, the knowledge of the local mass and momentum properties is of special interest. In general, the dispersion and the deposition of particles in turbulent flows is strongly influenced by interactions between flow geometry, particle sizes and flow velocity. To describe analytically the physics of particle migration in turbulent flows, theories have been developed in the past dividing the flow field near the walls into a viscous sublayer, a buffer region and a turbulent diffusion core region (see Friedlander & Johnstone 1957; Davis 1966). These theories differ by fundamental assumptions about the particle penetration in the sublayer and the particle deposition is explained by different concepts which are mostly based on inertia considerations. While micron-sized particles and fluid behave in a similar way in the core of a turbulent flow, it is commonly accepted that they act in a different way near the wall. Friedlander & Johnstone (1957) used a stopping distance concept which describes the transport of particles by eddies within one stopping distance from the wall where the particles coast to the wall due to their inertia. They assumed the particle diffusivity to be equal to the eddy diffusivity of the carrier gas, which is in contradiction to the work of Soo (1967), who found that the particle diffusivity is smaller than that of the carrier fluid. Rouhiainen & Stachiewicz (1970) based their

concept on the frequency response of particles in an oscillating flow field, see also Hjelmfelt & Mokros (1966). Trela (1982) presented a model of particle deposition from turbulent streams using a modified stopping distance concept which postulated equal probabilities for the particles to move toward the wall or back into the turbulent core. Also, Lee & Durst (1982) used a concept of particle frequency response in an oscillating flow field and introduced a simplifying model of particle response characterized by a cutoff frequency which allowed them to assess the ability of particles to follow the fluid oscillations. Some theoretical concepts have been compared with experimental results and are reported to be in good agreement (e.g. Kondić 1970; Trela 1982; Moujaes & Dougall 1985). Nevertheless, as far as particle behaviour near walls is concerned, controversies exist between the mostly theoretically deduced concepts, which can only be partially supported by experimental results. Furthermore, it is doubtful whether all of these concepts apply for separated flow regimes.

The particle dispersion and deposition in turbulent flows have been intensively investigated in experiments (e.g. Farmer *et al.* 1970; Simpson & Brolls 1974; Hetsroni & Sokolov 1971; Popper *et al.* 1974; Ruck & Pavlowski 1984; Lee & Börner 1987). Compared to the great number of experimental studies in particle-laden channel flows, detailed experimental investigations of the particle size-resolved dispersion in separated step flows are rare. This holds especially for the technically most relevant particle diameter range of 1–100 μm. The paucity of knowledge in this field is probably due to experimental and financial limitations. On the one hand, experimental on-line equipment to measure simultaneously individual particle sizes and velocities with a polydispersed size distribution in the flow (Bauckhage & Flögel 1984; Hishida *et al.* 1984; Ruck & Pavlowski 1984; Ruck *et al.* 1986) is not commonly in use and not trivial to apply. On the other hand, the costs for monodispersed particles, which can be advantageously used for size-dependent dispersion studies, are substantial.

To measure the particle velocities, laser-Doppler anemometry (e.g. Ruck 1987a, b) is an advantageous measuring method because the obtainable velocity information is directly related to the velocity of the individual particles suspended in the flow. Normal LDA applications infer the velocity information of a continuous fluid phase from the velocity data of small suspended particles. This can be done with a sufficient accuracy, as long as the particles are very small and ideally follow the flow fluctuations. If the particles increase in size, it is not the velocity of the continuous phase but the velocities of the individual particles which are measured. Thus, using monodispersed particles, one can measure the size-dependent particle dynamics, e.g. in a separated flow regime.

The investigations in this paper describe the dynamics of particles of different sizes in a single-sided backward-facing step flow. The particle diameters under investigation were 1, 15, 30 and 70 μm. It seemed reasonable to carry out the experiments with a 90°-step geometry, which represents the most commonly investigated and understood flow separation regime. The experiments were carried out for turbulent flow conditions.

GENERAL CONSIDERATIONS

To classify the aerodynamic behaviour of suspended particles in a carrier fluid, it is useful to define a parameter, which combines the viscous properties of the fluid as well as the inertia of the particle in the flow. Such a quantity can be derived from an equation set up according to Newton's second law, expressing the equilibrium between accelerating and drag forces in a stagnant fluid:

$$\frac{\mathrm{d}u}{u} = -\frac{9}{2} \cdot \frac{\eta}{r_\mathrm{p}^2 \cdot \rho_\mathrm{p}} \cdot \mathrm{d}t = \frac{1}{\tau} \cdot \mathrm{d}t, \qquad [1]$$

with u = particle velocity, η = dynamic viscosity of the fluid, ρ_p = density of the particle and r_p = radius of the particle. The quantity τ is referred to as the "relaxation time" of the particle and is commonly used to classify the aerodynamic properties of particles. The relaxation time expresses the ratio of the drag force of the carrier fluid to the inertia of the particles. Sometimes a stopping distance $x_\mathrm{s} = u_0 \cdot \tau$ is deduced to give a measure of the distance, a particle needs to stop in a specific environment, e.g. in the buffer region of a wall-bounded flow. Since many technical processes involve particles of non-spherical shape and different densities, it can be advantageous for comparisons to refer the particle size and shape-dependent results of the specific experiment to a

standard medium density of $\rho_0 = 1000\ \text{kg/m}^3$. Thus, an "aerodynamic diameter" d_a can be defined as

$$d_a = d_p \sqrt{\frac{C_p \rho_p}{C_0 \rho_0}}, \qquad [2]$$

with d_p = particle diameter, ρ_p = particle medium density and C_p and C_0 as Cunningham slip corrections for diameters in the range of the free molecular path length. The aerodynamic diameter d_a represents an equivalence diameter of a particle thought to have spherical shape and standard density which shows the same aerodynamic properties as the real particle under consideration.

The particles used in the experiments in this paper showed almost spherical shape, so that the introduction of an equivalence diameter was not chosen for the data presentation.

An analytical treatment of the particle movement in a turbulent flow can be performed by using the well-known Basset–Boussinesq–Ossen (BBO) equation:

$$\frac{du_p}{dt} = a(u_F - u_p) + b\frac{du_F}{dt} + c\int_{t_0}^{t} \frac{d(u_F - u_p)}{dT_0} \frac{dT_0}{(t - T_0)^{1/2}} + D, \qquad [3]$$

with u_p = particle velocity, u_F = fluid velocity and T_0 = convolution time interval. This equation describes the movement of a particle affected by a drag force originating from a difference in velocity between the particle and fluid, a term accounting for instantaneous instationary fluid velocity acceleration, a term which accounts for the flow history (convolution) and a term D which represents acting field forces such as gravity. For a comprehensive discussion of the BBO equation see Hinze (1959) and Sommerscales (1981).

For the description of the flow field, the stream function $\psi(y)$ can be computed for fixed values of y. In figure 1 a 90°-step geometry is sketched. The dividing streamline between the outer flow and the recirculation zone is defined by $\psi(y) = 0$. That means roughly that the hatched areas of positive and negative velocities inside the recirculation zone correspond to each other. Another typical describing quantity is the zero velocity line $u = 0$ in the separation region. Both, the dividing streamline and the zero velocity line coincide at the point of separation and reattachment of the flow. Thus, the reattachment point x_R is characterized by a time-averaged velocity of zero. In analogy to the stream function, a quantity ϕ has been introduced by some experimenters to express the streamwise turbulent intensity in the cross-section under investigation:

$$\phi = \int_0^{y_{max}} u'(y)\, dy, \qquad [4]$$

with $u'(y)$ as the turbulent fluctuation or r.m.s. velocity. The integral is normally extended over the whole cross-section. Whereas $\psi(y)$ integrated over the cross-section must be constant for all locations (x-positions) and reflecting the continuity law, ϕ is a specific local turbulence characterizing quantity which does not remain constant, but changes significantly with the wall geometry.

In the following, the results of the experimental investigations are expressed in the above-mentioned terms. Local positions and lengths are made dimensionless with the step height of the step flow.

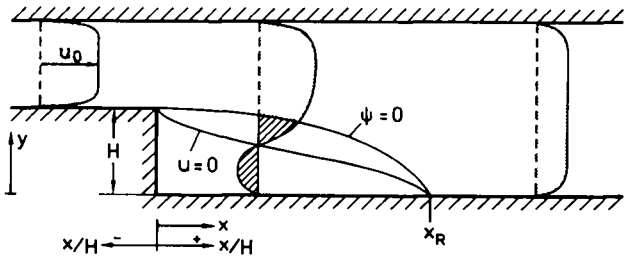

Figure 1. 90° backward-facing step geometry; $\psi = 0$ dividing streamline; $u = 0$ zero velocity line.

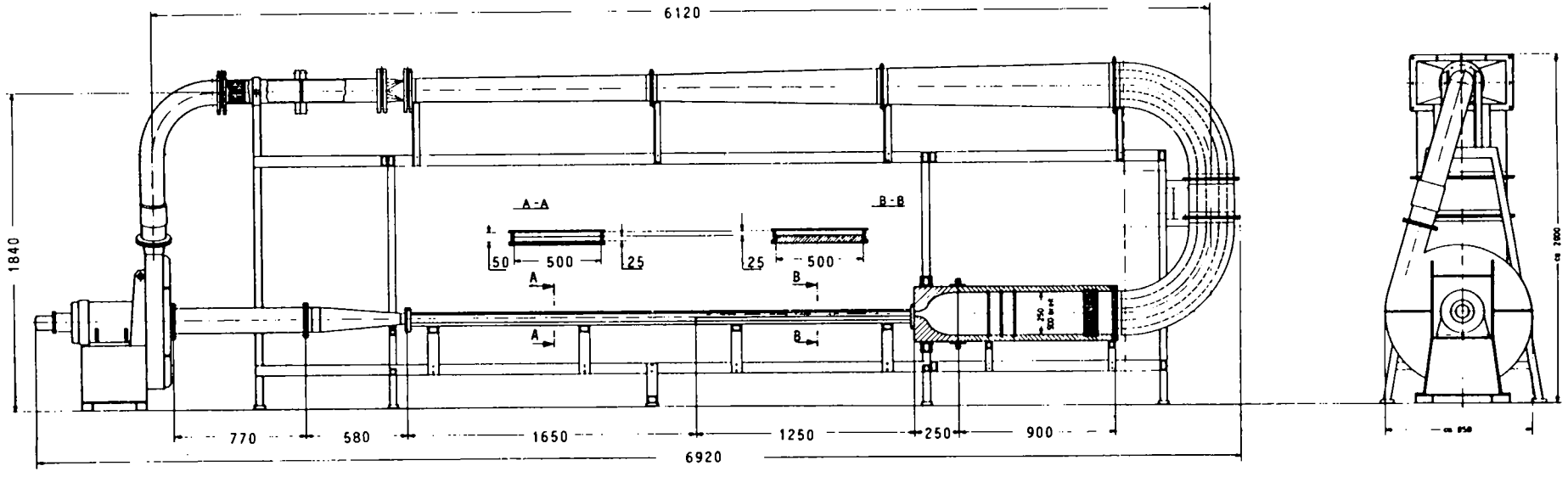

Figure 2. Closed-loop wind tunnel with glass test section (dimensions in mm).

EXPERIMENTAL APPARATUS

For the experiments, a closed-loop wind tunnel was used. The wind tunnel (figure 2) had a test section made of glass. An expansion ratio of 1:2 and a length of 116 step heights were realized. The inner width of the test section was 500 mm, the step height was 25 mm and the channel height after the step was 50 mm. The dimensions of the inlet length of the test section were calculated to ensure fully-developed flow conditions at the step with respect to vertical and lateral profile symmetry, mean flow and turbulent quantities. This can be inferred from figure 3, which gives the mean velocity and r.m.s. velocity profiles before the step at different locations with a Reynolds number (formed with step height H) $Re_H = 43{,}000$. The wind tunnel was driven by a fan, which allowed us to realize flow velocities up to 50 m/s and which is equivalent to $Re_H \leqslant 10^5$.

MEASURING TECHNIQUE

The local particle velocity was measured using a conventional one-dimensional LDA. Since the step geometry was set up to yield a two-dimensional flow, the used one-dimensional LDA system delivers only limited flow information. Nevertheless, the integral flow describing quantities, reattachment lengths, zero velocity lines and separation streamlines, could be measured precisely. The LDA measures the velocity of, from a more general point of view, changing refractive index interfaces moving through the measuring volume, i.e. the measuring point formed by at least two incident laser beams. The LDA system, driven by a 15 mW He–Ne laser, was working in the forward light scattering direction. The system was equipped with a double Bragg cell arrangement to discriminate the flow direction and to resolve regions of recirculation. The diameter of the LDA-measuring volume was chosen as 500 μm. The half-angle of the crossing laser beams was 2.86°, which corresponds to a fringe spacing of $\Delta x = 6.33\ \mu$m.

Figure 4 shows the LDA mounted on a traversing unit. The measurements were based on a single particle velocity evaluation. The data evaluation was performed by a 100 MHz transient recorder with software processing in an associated microcomputer.

PARTICLE SEEDING

The flow field investigations were carried out with an LDA which requires the existence of light scattering particles in the flow. For some measurements, e.g. in water flows, natural impurities in the fluid sometimes suffice to apply this advantageous non-intrusive measuring technique. Normally, the flow has to be seeded with particles to measure the flow field. If small submicron-sized particles are used which follow the flow fluctuations ideally, the LDA yields the flow velocity information of the continuous phase. To trace the continuous fluid phase in the experiments small oil droplets of a median dia $d_p \cong 1\ \mu$m were used. The oil droplets were generated by an atomizer with associated impactors to separate bigger droplets. The diameter of the oil droplets was

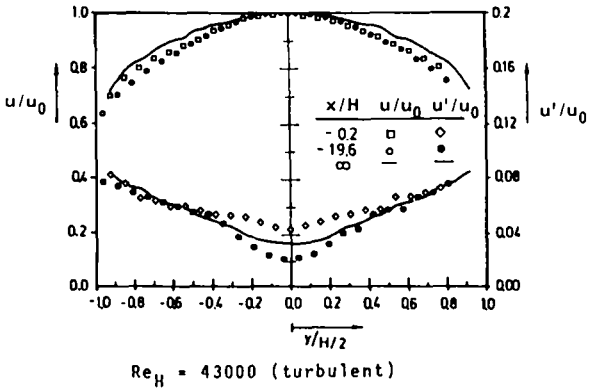

Figure 3. Mean velocity and r.m.s. velocity profiles before the step at different locations (x = streamwise position, y = vertical position, H = step height).

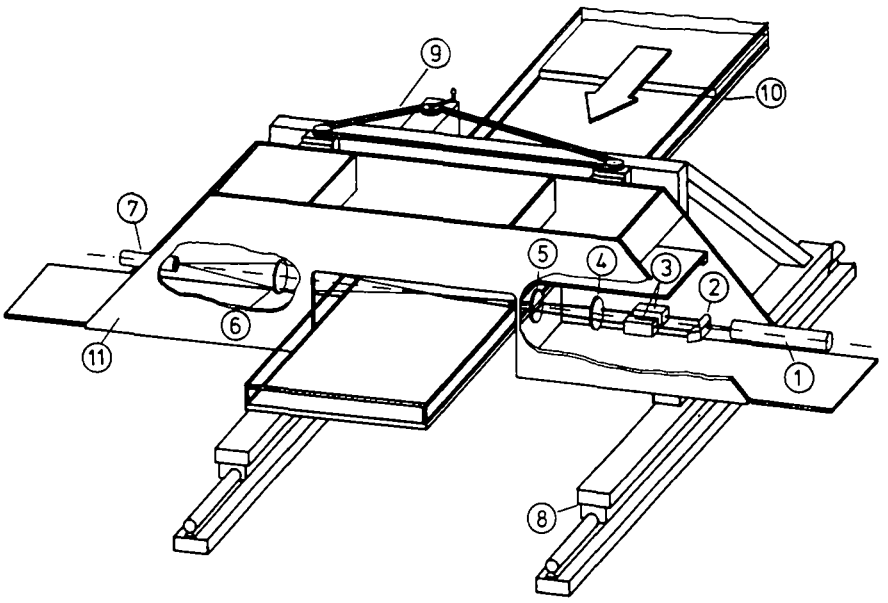

1	Laser	6	Lens
2	Beam Splitter	7	Photomultiplier
3	Bragg cells	8	Longitudinal displacement
4	Lens	9	Vertical displacement
5	Mask	10	Test section (step)
		11	Test rack

Figure 4. Laser-Doppler anemometer mounted on a traversing unit.

additionally controlled by an optical particle-sizing system (see Ruck & Pavlowski 1984). The density of the oil was $\rho = 810\,\mathrm{kg/m^3}$.

For the investigation of the dynamics of differently sized particles, starch particles of almost uniform size were used. The density of the particle medium is $\rho = 1500\,\mathrm{kg/m^3}$. The particles show a spherical shape and are not soluble in cold water. Figure 5 is a photograph of 50 μm dia starch particles, taken by electron microscopy.

Three different size classes 15, 30 and 70 μm dia, were chosen for the systematic experimental investigations in the backward-facing step flow. The particles were injected into the wind tunnel after the radial fan. The injection was performed by a special device based on premixing of the particles in a pressurized tank. The normal loss of suspended particles due to wall deposition was compensated by a permanent low seeding rate. Degradation of the particles was not observed. Table 1 gives a compilation of the particles used in the experiments.

It should be mentioned that the particle number concentration in the experiments was relatively low (10^2–$10^3/\mathrm{cm^3}$), so that the influence measured was that of the flow on the particle movement and not that of the particles on the flow. In this concentration and size range, the distortion of the flow field by particles is negligible.

RESULTS

The following results represent time-averaged flow velocities and turbulence data. It should be remarked that the actual local mean data are ensemble-averaged quantities, which rely on 1000 single LDA bursts. As mentioned before, the signal processing was performed by a transient recorder–microcomputer combination. The processable data rate was about 10 readings/s which is rather low and predominantly caused by the data handling between recorder and computer. Together with a sufficiently high particle number concentration, a periodic sampling of the information was induced. It was not the particle arrival rate in the measuring volume, but the time to process the data which determined the data rate. There is no evidence for further analytical corrections with bigger particles, as long as it can be ensured that whenever the data processor is

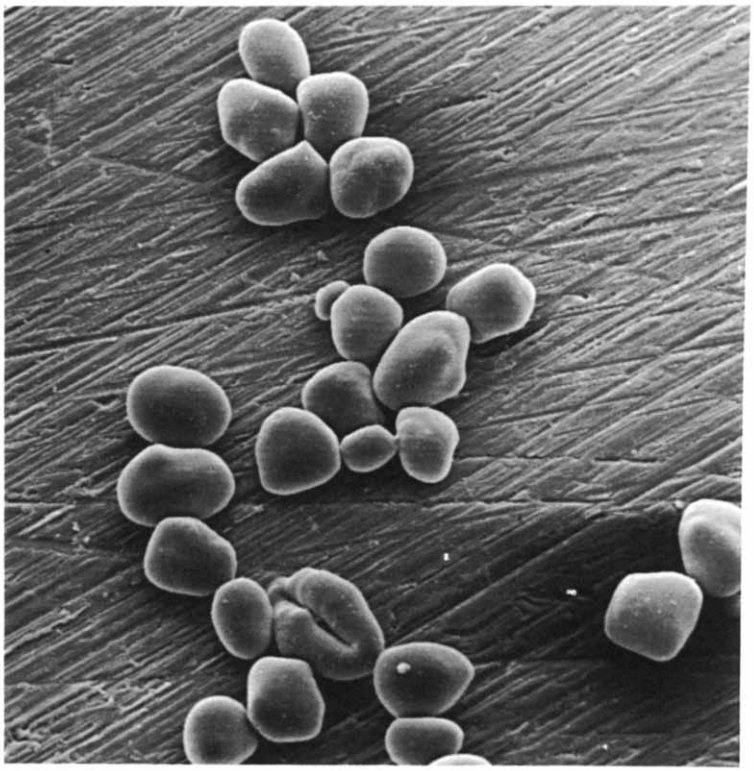

Figure 5. Starch particles of 50 μm dia under the electron microscope.

ready to evaluate, a signal is supplied instantaneously. Thus, biasing effects did not occur because the periodic sampling equalized the differences between ensemble- and time-averaged data information.

Figure 6 shows two series of mean velocity profiles after the single-sided step for oil particles of 1 μm dia and starch particles of 70 μm dia. It can be inferred that the 70 μm particles show smaller recirculating velocities than the 1 μm particles. Furthermore, a smaller recirculation zone would be inferred from the velocity profile of the larger particles. As a trend, all the experiments deliver higher positive values for bigger particles in all the cross-sections under investigation. Figure 7 gives the corresponding r.m.s. velocities to figure 6. The maximum r.m.s. values of bigger particles are shifted more towards the lower wall. This indicates, that the particle fluctuations caused by the free shear layer are influenced by gravity in that particle size range. Furthermore, the significant cross-sectional bimodal r.m.s. velocity distribution in the free shear layer is damped for bigger particles.

Big particles suspended in a flow have a higher momentum, which leads to a longer stopping distance when the continuous flow is slowed down, e.g. by an expansion of the channel geometry. This can be seen in figure 6, where the streamwise local mean velocities stay at a higher level longer for the 70 μm particles than for the smaller ones. For $u = 40$ m/s the corresponding stopping distances were 10^{-4} m for 1 μm particles and 0.9 m for 70 μm particles, respectively.

Table 1. Diameter and relaxation time of suspended particles at 20°C

Particle media	d (μm)	$\tau \cdot 10^6$ (s)
Oil	1	2.51
Starch	15	1047
Starch	30	4190
Starch	70	22811

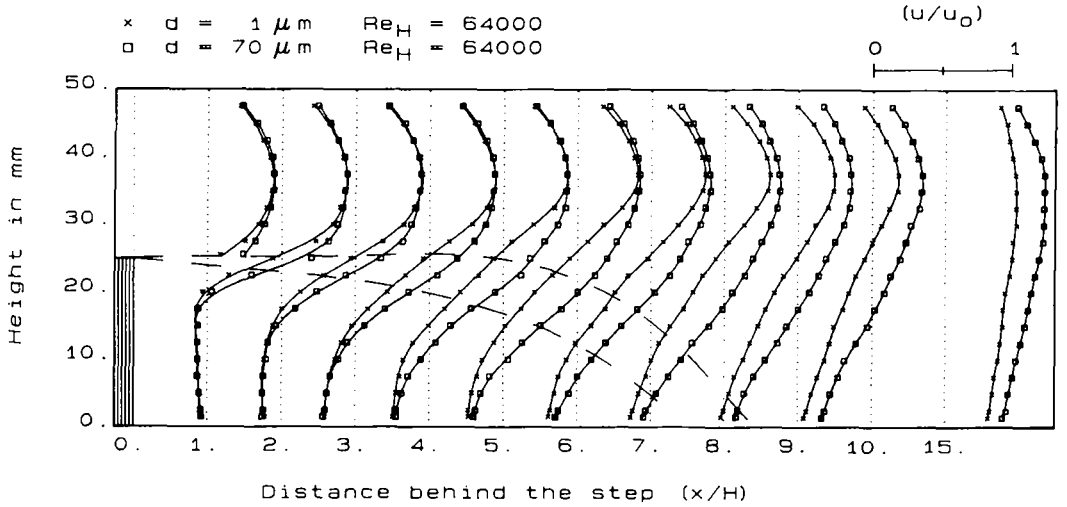

Figure 6. Mean velocity profiles for 1 and 70 μm particles behind the backward-facing step with $Re_H = 64{,}000$.

Besides the changes in the particle velocity due to different particle size, the velocity field is additionally Reynolds number dependent. Figure 8 shows the particle velocity profiles for 70 μm particles with two different Reynolds numbers, 15,000 and 64,000. In agreement with existing results of single-phase separated flows documented in the literature, a higher recirculation velocity was registered for a higher streamwise velocity, e.g. Reynolds numbers. As can be seen in figure 8, this led to an increase in reattachment length of the particle flow. The higher momentum of the particles with $Re = 64{,}000$ is reflected in the higher streamwise velocities in the cross-sections behind the step. Even in a distance of 15 step heights from the step, the mean normalized velocity profiles do not yet coincide. The corresponding turbulent intensity is given in figure 9. The difference in r.m.s. velocities is small up to $x/H \cong 3$. Near the reattachment position of the particle flow the differences show a maximum. The flow with $Re = 64{,}000$ had higher r.m.s. velocities in almost all the cross-sections investigated.

A comparison of figures 6 and 7 with figures 8 and 9 reveals that the more significant changes in particle velocity profile stem from the change in particle size rather than from Reynolds number variations. The asymmetry in the turbulent intensity profiles in figures 7 and 9 seems also to be strongly particle size dependent.

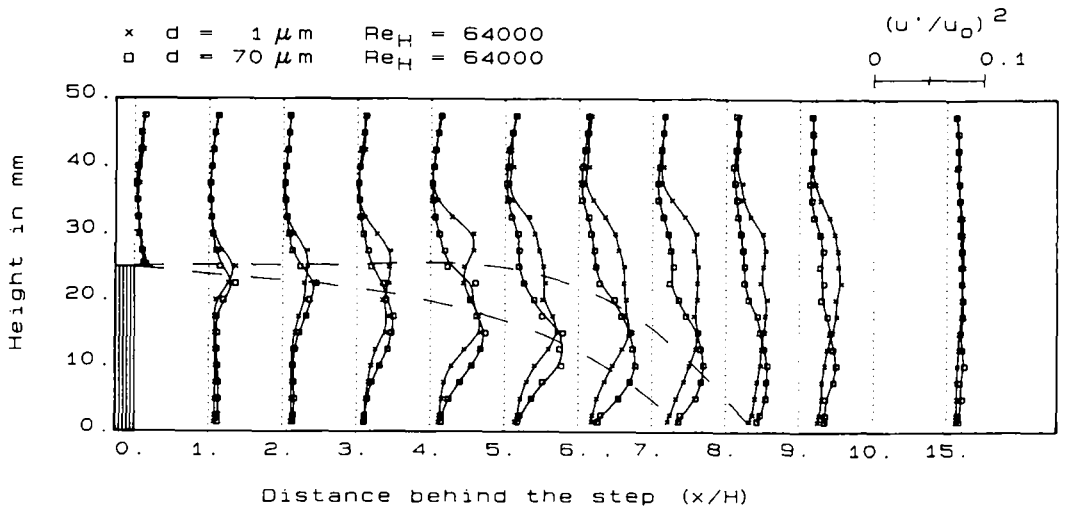

Figure 7. r.m.s. velocity profiles for 1 and 70 μm particles behind the step; see figure 6.

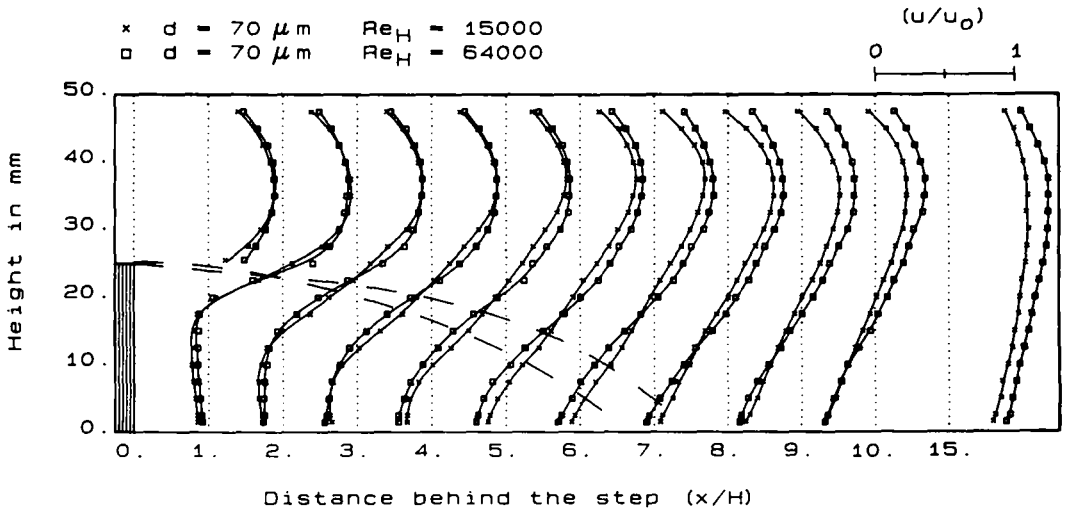

Figure 8. Mean velocity profiles for 70 μm particles behind the backward-facing step with two different Reynolds numbers, Re = 15,000 and 64,000.

In figures 10 and 11 the maximum positive streamwise and negative counterstreamwise velocity for the velocity profile considered is given. The aforementioned particle dynamics are reflected well in these graphs. It can be inferred that up to position $x/H \cong 3$ no significant changes between the particle velocities in the streamwise and recirculation direction can be observed. The differences in particle velocity data begin to grow behind $x/H \cong 3$. The position of the maximum negative velocity in the separation zone is shifted to slightly smaller values of x/H with increasing particle size, but still remains around $x/H \cong 4$.

As we have seen before, the particle velocity data of different particle classes deviate from each other and the trends with increasing sizes are obvious. If this information is used to describe the flow field, different velocity profiles will result. In figure 12, the dividing streamline and line of streamwise zero velocity are shown for all particle size classes investigated and a Reynolds number of $Re_H = 15{,}000$. The reattachment length of the particle velocity field is effectively shortened with increasing particle diameter. This suggests that in separated flow regions the use of particle-related measuring techniques can lead to erroneous measurements, when the particulate phase is not controlled with respect to the size classes involved. The experiments show clearly that a distinction between flow velocity field and particle velocity field has to be made in separated flow regions even in the particle size range of micrometers.

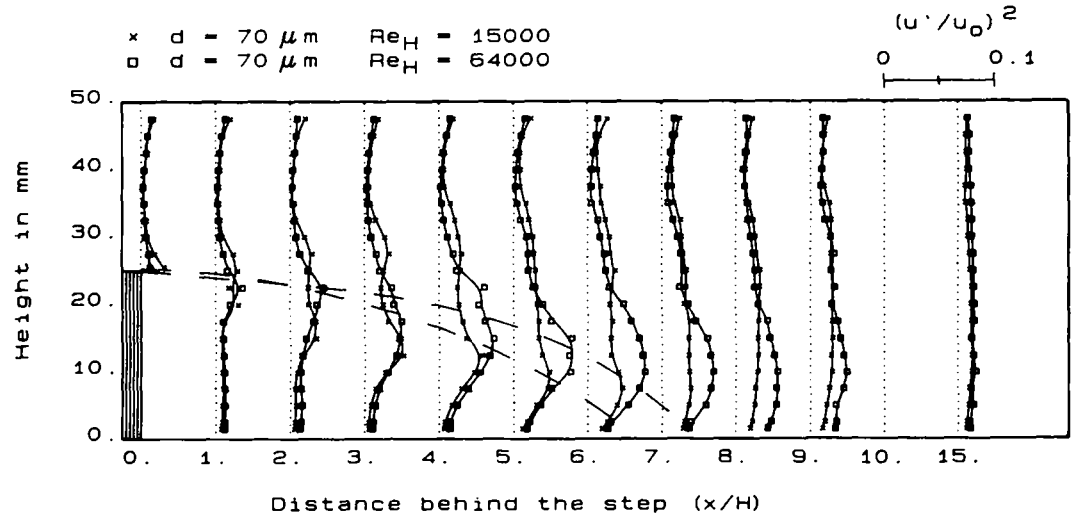

Figure 9. r.m.s. velocity profiles for 70 μm particles behind the step; see figure 8.

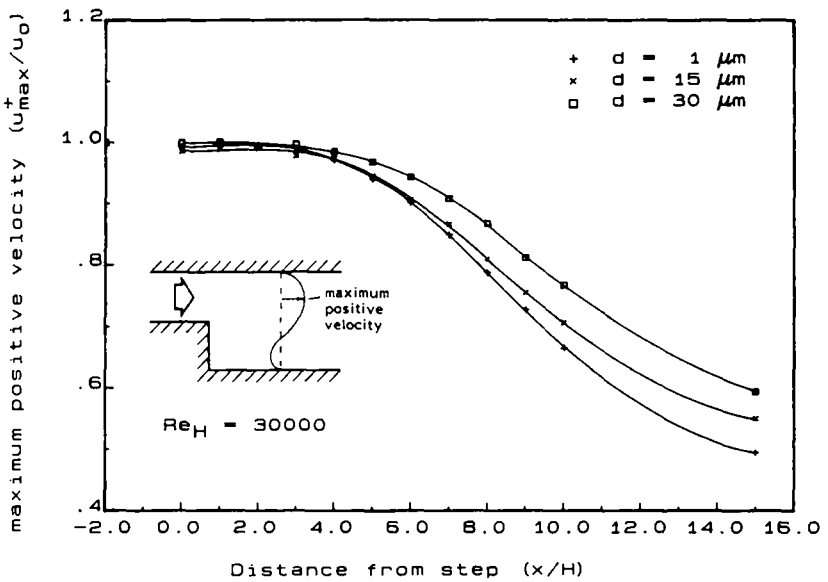

Figure 10. Maximum positive velocity u^+_{max} (normalized with u_0) in the streamwise portion of the velocity profile of particles of different sizes.

To assess the influence of tracer particle size on the accuracy in LDA measurements, the cross-sectional volume flux (ψ_{ges}), derived from the LDA information of the different size classes involved, was determined throughout the flow. To estimate the deviation of the particle phase flow and the continuous phase flow, $\psi_{ges}(x/H)$ for each particle velocity profile was calculated and normalized with $\psi_{ges}(x/H = -2)$ two step heights before the step, where the flow is still undisturbed. The results at Reynolds number $Re_H = 64{,}000$ and different particle sizes are shown in figure 13. The corresponding cross-sectional integrated r.m.s. velocities are given in figure 14. The normalized volume flux derived from differently sized particles in the undisturbed and developed flow before the step show the same values for the entire particle range investigated and all Reynolds numbers. Behind the expansion, the ψ_{ges}-values for the starch particles increase with increasing particle diameter and Reynolds number. The maximum values for all starch particles are reached at $x/H \cong 8$–9. Thereafter ψ_{ges} decreases slowly. The ψ_{ges}-values based on larger particles

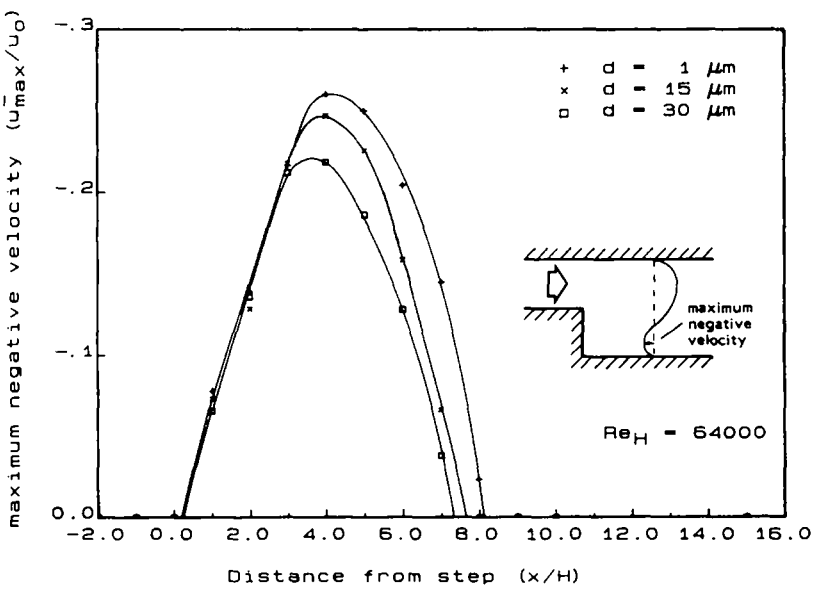

Figure 11. Maximum negative velocity u^-_{max} (normalized with u_0) in the recirculation zone of particles of different sizes.

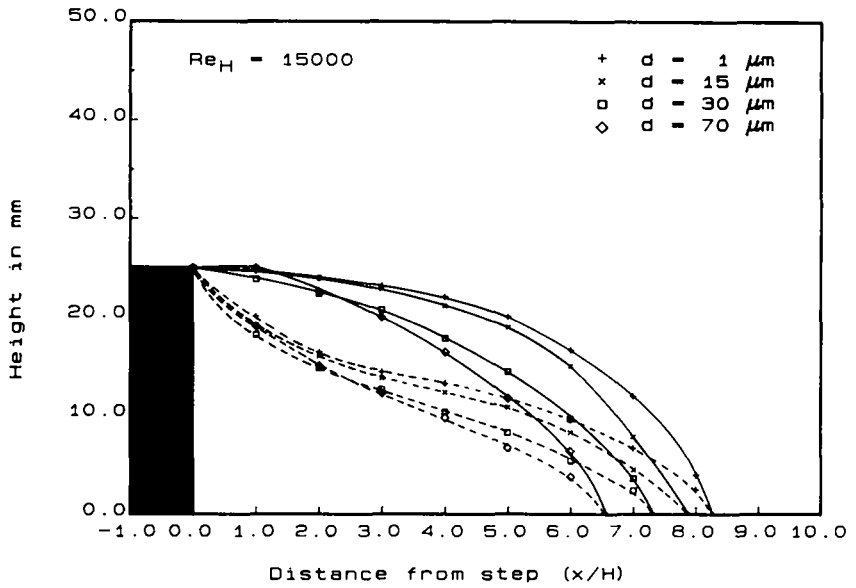

Figure 12. Dividing streamline (———) and line of streamwise zero velocity (— — —) derived from particle velocities of particles of different sizes.

lead to an increase in measured volume flux (a contradiction to the continuity law) behind the step and deviations of more than 40% from the upstream values at $Re_H > 45{,}000$ and 70 μm particle diameter have been registered. The ψ_{ges}-values from oil droplets show only small deviations, an order of magnitude smaller than that derived from the starch particles. It can be clearly seen that the delayed momentum decay of big particles can lead to erroneous measurements of continuous-phase flow quantities.

The results given in figures 6–14 indicate that flow separation induces particle size class dependent phenomena. If polydispersed particle size distributions are suspended in a flow with separation, another factor has to be considered, which is the problem of size class separation and which is highly relevant for the application of flow velocity measuring techniques. The particles not only behave in the described way with respect to their velocity information, but also their number concentration differs depending on the size class and flow field region. This is shown in

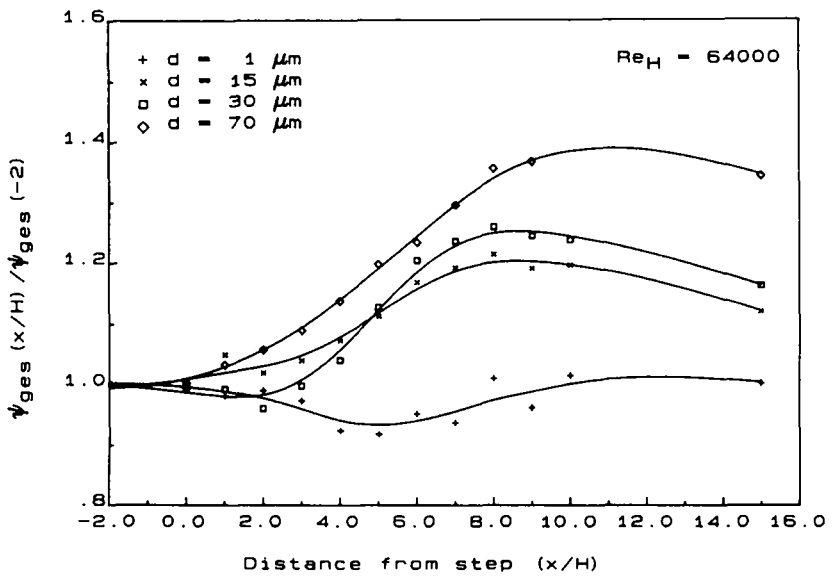

Figure 13. Normalized volume flux (ψ_{ges}) derived from differently sized particles behind the step at $Re_H = 64{,}000$.

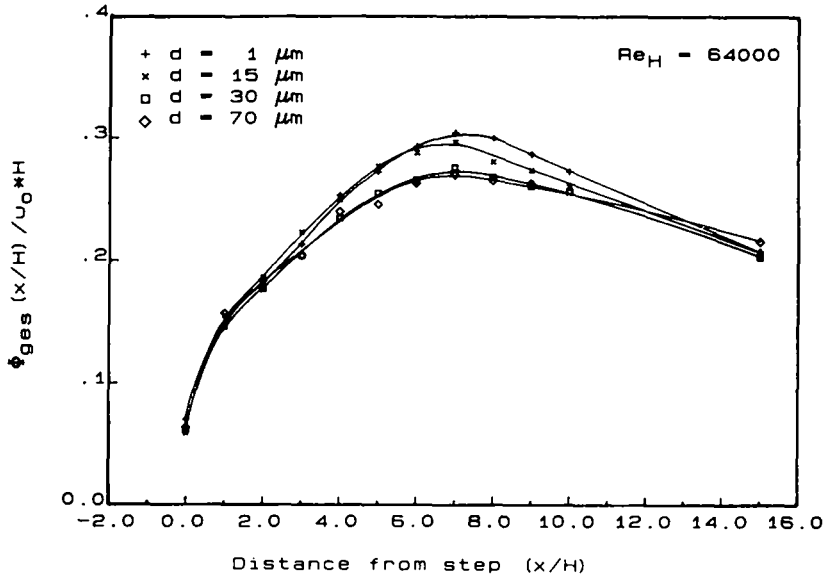

Figure 14. Integrated r.m.s. velocities over the cross-section of differently sized particles.

figure 15 for the same step flow geometry, where in a cross-section before and behind the step successive particle size measurements were carried out, with a white-light particle-sizing system. The particle size distributions given in the cumulative percentage curves show that in the separation region significantly fewer bigger particles exist when compared to the distribution of the approach flow.

CONCLUSIONS

The paper presents measured data of particle dynamics in a backward-facing step flow with separation. Particles of 1, 15, 30 and 70 μm dia were suspended in the flow and traced by the optical

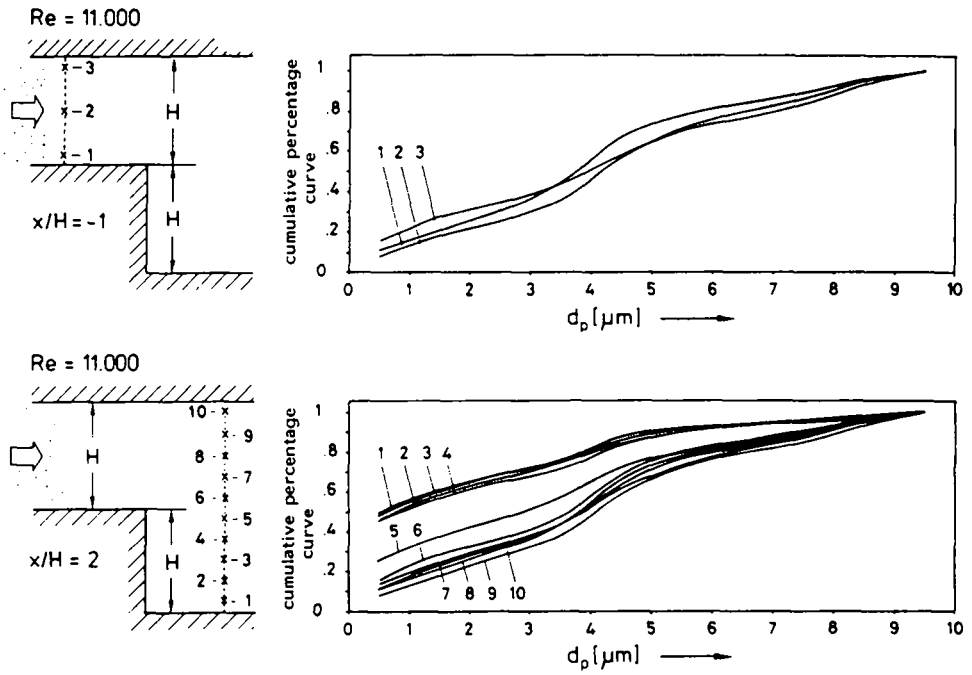

Figure 15. Differences in particle size distributions at different locations before and behind a step.

non-intrusive LDA technique. The results show that with increasing particle size, the particle velocity field differs increasingly from the flow velocity field of the continuous phase. For bigger particles, the velocity fluctuations in all the cross-sections under investigation decrease. In the zone of recirculation, big particles give a lower velocity than small ones. The opposite holds for the streamwise portion of the velocity field, where big particles have a higher velocity in the cross-sections near the step. If derived from particle velocity information, the dimensions of the recirculation zone decrease with increasing particle size. This is due to the reduction of negative counterstreamwise particle velocities in the separation region, which effectively shortens the measured reattachment length. Comparing the results of differently sized particles in the flow, it can be inferred that particle diffusion differs from the eddy diffusion even in the range of micron-sized particles. Additionally, the results demonstrate the dependence of particle sizes on flow data, when particle-related measuring techniques are used.

Acknowledgements—This work was supported by the Deutsche Forschungsgemeinschaft under Grant No. Ru 345/2. The support is gratefully acknowledged. The authors would also like to express their thanks to Paul Wieland for assisting in the measurements, to Mrs D. Bring for typing the manuscript and to Mr Schumacher from KSL GmbH/Lauingen, F.R.G., for his friendly cooperation.

REFERENCES

ABBOTT, D. E. & KLINE, S. J. 1962 Experimental investigation of subsonic turbulent flow over single and double backward-facing steps. *Trans. ASME Jl Basic Engng* 317–325.

ADAMS, E. W. & JOHNSTON, J. P. 1988 Effects of the separating shear layer on the reattachment flow structure, Part 1: pressure and turbulence quantities; Part 2: reattachment length and wall shear stress. *Exps Fluids* **6**. In press.

ARMALY, B. F., DURST, F., PEREIRA, J. C. F. & SCHÖNUNG, B. 1983 Experimental and theoretical investigation of backward-facing step. *J. Fluid Mech.* **127.**

BAUCKHAGE, K. & FLÖGEL, H. H. 1984 Simultaneous measurement of droplet size and velocity in nozzle sprays. *Proc. 2nd Int. Symp. on Applications of Laser Anemometry to Fluid Mechanics*, Chap. 18.1, Lisbon.

BRADSHAW, P. & WONG, F. Y. 1972 The reattachment and relaxation of a turbulent shear layer. *J. Fluid Mech.* **52.**

DAVIES, C. N. 1966 Deposition of aerosols through pipes. *Proc. R. Soc. A* **289,** 235–246.

FARMER, R., GRIFFITH, P. & ROHSENOW, W. M. 1970 Liquid droplet deposition in two-phase flow. *J. Heat Transfer* 587–594.

FRIEDLANDER, S. K. & JOHNSTONE, H. F. 1957 Deposition of suspended particles from turbulent gas streams. *Ind. Engng Chem.* **49,** 1151–1156.

HETSRONI, G. & SOKOLOV, M. 1971 Distribution of mass, velocity, and intensity of turbulence in a two-phase turbulent jet. *J. appl. Mech.* 315–327.

HINZE, J. O. 1959 *Turbulence*. McGraw-Hill, New York.

HISHIDA, K., TAJIMA, K. & MAEDA, M. 1984 Measurement of two-phase turbulent flow by LDA with particle size discrimination. *Proc. 2nd Int. Symp. on Applications of Laser Anemometry to Fluid Mechanics*, Chap. 18.4, Lisbon.

HJELMFELT, A. T. & MOKROS, L. F. 1966 Motion of discrete particles in a turbulent fluid. *Appl. scient. Res.* **16,** 149–161.

KONDIĆ, N. N. 1970 Lateral motion of individual particles in channel flow—effect of diffusion and interaction forces. *J. Heat Transfer* **92,** 418–428.

LEE, S. L. & DURST, F. 1982 On the motions of particles in duct flows. *Int. J. Multiphase Flow* **8,** 125–146.

LEE, S. L. & BÖRNER, T. 1987 Fluid flow structure in a dilute turbulent two-phase suspension flow in a vertical pipe. *Int. J. Multiphase Flow* **13,** 233–246.

MOUJAES, S. & DOUGALL, R. S. 1985 Two-phase upflow in rectangular channels. *Int. J. Multiphase Flow* **11,** 503–513.

NAKAGAWA, H. & NEZU, I. 1987 Experimental investigation on turbulent structure of backward-facing step flow in an open channel. *J. Hydraul. Res.* **25,** 67–89.

POPPER, J., ABUAF, N. & HETSRONI, G. 1974 Velocity measurements in a two-phase turbulent jet. *Int. J. Multiphase Flow* **1**, 715–726.

ROUHIAINEN, P. O. & STACHIEWICZ, J. W. 1970 On the deposition of small particles from turbulent streams. *J. Heat Transfer* **92**, 169–177.

RUCK, B. 1987a Laser Doppler anemometry—a non-intrusive optical measuring technique for fluid velocity. *Particle Character.* **4**, 26–37.

RUCK, B. 1987b *Laser-Doppler-Anemometrie*. AT-Fachverlag, Stuttgart.

RUCK, B. & PAVLOWSKI, B. 1984 Kombinierte optische Messung von Teilchengrößen-und Teilchengeschwindigkeitsverteilungen im Rohr. *Tech. Messen Jber.* **2**, 61–67.

RUCK, B., SCHMITT, F. & LOY, T. 1986 Particle dynamics in a separated step flow. *Proc. 3rd Int. Symp. on Application of Laser-Anemometry to Fluid Mechanics*, Chap. 2.1, Lisbon.

SCHMITT, F. 1987 Untersuchung der turbulenten Stufenströmung bei hohen Reynoldszahlen. *Fortschr. Ber. VDI* **117**(7), (Dissertation).

SIMPSON, H. C. & BROLLS, E. K. 1974 Droplet deposition on a flat plate from an air–water mist in turbulent flow over the plate. *Symp. on Two-Phase Flow Systems*, Vol. 1 (A3), University of Strathclyde, Glasgow.

SOMMERSCALES, E. F. C. 1981 *Tracer Methods, Fluid Dynamics*, Part A (Edited by EMRICH, R. J.). Academic Press, New York.

SOO, S. L. 1967 *Fluid Dynamics of Multiphase Systems*. Blaidsell, Waltham, Mass.

TRELA, M. 1982 Deposition of droplets from turbulent stream. *Wärme. Stoffübertrag.* **16**, 161–168.